GeoScienceEd *7(3) (2026)*

Jurnal Pendidikan, Sains, Geologi, dan Geofisika

http://jpfis.unram.ac.id/index.php/GeoScienceEdu/index

Convective Rainfall Z-R Equation Characteristics for C-Band Weather Radar in the Jakarta Region

Muhammad Fadhillah[1], Yosafat Donni Haryanto[1*], Purwanti Lelly Sabrina[1], Dodo Gunawan[2]

[1] Meteorology Study Program, College of Meteorology, Climatology, and Geophysics (STMKG), Tangerang, Banten, Indonesia.
[2] Climatology Study Program, College of Meteorology, Climatology, and Geophysics (STMKG), Tangerang, Banten, Indonesia.

DOI: https://doi.org/10.29303/goescienceed.v7i3.2661

Article Info:
Received : May, 28 2026
Revised : June, 16 2026
Accepted : June, 27 2026
Published : July, 29 2026

Correspondence:

Yosafat Donni Haryanto

Phone: +628111541585

Abstract: Operational quantitative precipitation estimation (QPE) from the C-Band weather radar in Jakarta still relies on the generic Marshall-Palmer (Z=200R^1.6) and Rosenfeld Tropical (Z=250R^1.2) Z-R relationships, neither calibrated to the local Drop Size Distribution (DSD) of convective rainfall in this tropical maritime region. This study aimed to derive a locally modified Z-R coefficient specific to convective rain, defined as rain rate ≥10 mm/hour, using a statistical regression optimization approach. Volumetric raw data (.vol) from the Tangerang C-Band radar were paired with hourly rainfall records from 32 automatic rain gauges (ARG and AWS) within a 50 km radius during January–April 2024, following Column Maximum (CMAX) extraction and quality control procedures. Linear regression on log-transformed reflectivity and rainfall data yielded a new convective equation, Z=152R^1.4, with a correlation coefficient of 0.6972 and coefficient of determination of 0.4861. These moderate values are consistent with the naturally wide Drop Size Distribution spectrum of convective rainfall, rather than indicating a weak physical relationship between reflectivity and rain rate. Taylor Diagram verification showed the new equation sustaining a correlation of approximately 0.95, close to observed variability, with root mean square error near 3.9 dBZ, outperforming Marshall-Palmer and Rosenfeld Tropical in balancing correlation and standard deviation under convective conditions. These findings support operational adoption of a locally derived convective Z-R relationship for Jakarta's radar-based rainfall estimation.

Keywords: Z-R Relationship; Convective Rainfall; C-Band Radar; Drop Size Distribution; Quantitative Precipitation Estimation

Citation: Fadhillah, M., Haryanto, Y. D., Sabrina, P. L., & Gunawan, D. (2026). Convective Rainfall Z-R Equation Characteristics for C-Band Weather Radar in the Jakarta Region. *Jurnal Pendidikan, Sains, Geologi, Dan Geofisika (GeoScienceEd Journal)*, *7*(3), 4533–4539. https://doi.org/10.29303/goescienceed.v7i3.2661

Introduction

Jakarta's dense urban core experiences some of the most spatially concentrated and intense rainfall events recorded in the Indonesian tropics, and this concentration translates directly into elevated flood risk whenever convective cells develop over the city and its surrounding catchments (Kusuma & Wardoyo, 2018). Point-based rain gauge networks remain the primary ground-truth instrument for rainfall measurement, yet their sparse spatial coverage limits the ability to resolve rainfall variability across a metropolitan area of this scale (Kidd et al., 2017). Weather radar addresses this gap through continuous, wide-area observation of precipitation structure, which positions C-Band radar as a central instrument for operational rainfall monitoring across the Jakarta region. The stakes of this gap extend beyond statistics into operational consequence. An underestimation error approaching 10 mm/hour, a magnitude already documented for uncalibrated Z-R equations applied to convective rainfall in Jakarta

Email: yosafat.haryanto@stmkg.ac.id

(Kusuma & Wardoyo, 2018), is sufficient to keep a flood early warning system below its alert threshold during a genuine high-intensity event. In a dense urban catchment where surface runoff response is measured in minutes rather than hours, this margin of error translates into a delayed mitigation response at precisely the moment when lead time matters most.

Radar systems do not measure rainfall directly. Instead, they record the reflectivity (Z) of backscattered energy from hydrometeors, a quantity converted into rain rate (R) through an empirical power-law relationship of the form $Z = AR^b$, commonly referred to as the Z-R relationship (Lakkham, 2017). This conversion underlies the process known as Quantitative Precipitation Estimation (QPE). Because the coefficients A and b are governed by the Drop Size Distribution (DSD) of the precipitation being sampled, and DSD itself varies with climatic regime and storm microphysics, a Z-R equation calibrated for one region carries no guarantee of accuracy when applied elsewhere (Dhiram & Wang, 2016; Gou & Chen, 2021).

Operational practice at the Tangerang C-Band radar, which serves the Jakarta metropolitan area, still relies on two globally referenced formulations, Marshall-Palmer ($Z = 200R^{1.6}$) and Rosenfeld Tropical ($Z = 250R^{1.2}$), neither of which was derived from local DSD observations. Repeated evaluations within Indonesian territory point to the resulting mismatch: Kusuma and Wardoyo (2018) reported that Marshall-Palmer estimation error for Jakarta rainfall reached a mean of -9.8 mm/hour under convective conditions, a magnitude considerably larger than the error recorded for stratiform events using the same equation. Talumassawatdi et al. (2016) documented a comparable sensitivity of Z-R performance to local calibration in Thailand, where regionally derived coefficients improved estimation accuracy by 10-30% relative to standard formulations.

The discrepancy is most pronounced for convective rainfall. Convective precipitation forms through strong, localized updrafts capable of exceeding several meters per second, an environment in which collision-coalescence and droplet breakup operate simultaneously and at high efficiency (Syafira et al., 2021; Notaroš et al., 2022). The resulting DSD spectrum is markedly broader and more variable in space and time than the DSD associated with the slower, thermodynamically stable growth processes typical of stratiform rain. A single empirical Z-R regression is inherently limited in its capacity to represent this variability, a constraint that Biondi et al. (2024) identify as a structural rather than incidental weakness of regression-based QPE under convective conditions. Convective rainfall therefore poses the more demanding calibration challenge of the two rain types and remains the larger source of estimation uncertainty for radar-based QPE in tropical maritime regions such as Jakarta.

Modern radar processing suites, including the Stratiform-Convective Classification module built into Rainbow 5 software, are technically capable of separating precipitation types in real time, but this capability becomes operationally useful only once region-specific A and b coefficients are supplied for each rain category (Romatschke & Dixon, 2022; Mocva-Kurek et al., 2025). Direct DSD measurement through disdrometer networks would satisfy this requirement, yet the limited distribution of such instruments across Indonesia makes statistical regression between radar reflectivity and rain gauge observations the more practical calibration pathway (Sahlaoui & Mordane, 2019; Hutapea et al., 2021). Despite this precedent, no published Z-R coefficient specific to convective rainfall has yet been derived for the Tangerang radar's operational coverage of Jakarta and its surrounding area.

This study addresses that gap by deriving a locally modified Z-R equation for convective rainfall, defined here as rain rate ≥10 mm/hour, using volumetric reflectivity data from the Tangerang C-Band radar paired with automatic rain gauge observations collected between January and April 2024. The derived equation is evaluated against the Marshall-Palmer and Rosenfeld Tropical formulations through Taylor Diagram verification, with the aim of determining whether a regionally calibrated convective coefficient yields measurable improvement in correlation and variability representation over the equations currently used in BMKG's operational radar practice.

Method

Research Design

This study follows a quantitative, experimental-comparative design. The experimental component involves deriving a modified Z-R coefficient through statistical regression, treating hourly rain gauge intensity as the independent variable and radar reflectivity as the dependent variable from which the new equation is generated. The comparative component follows once the modified coefficient is obtained, evaluating its performance against the two standard formulations currently used in operational practice, Marshall-Palmer ($Z = 200R^{1.6}$) and Rosenfeld Tropical ($Z = 250R^{1.2}$), using correlation coefficient, standard deviation, and root mean square error as the basis for comparison.

Study Area and Data Period

The research domain covers a 50 km radius around the C-Band weather radar located at Soekarno-Hatta Class I Meteorological Station, Tangerang, a coverage area that encompasses Jakarta and its adjacent metropolitan districts. This radius sits within the effective operating range for C-Band systems identified by Bringi and Hendry (1990), who set 100 km as the upper limit for reliable signal return. Data collection was restricted to rainfall events recorded simultaneously by the radar and the automatic gauge network across the period of January to April 2024. Of the 32 candidate stations within this radius, 19 were eliminated due to radar-geometry limitations (17 due to the cone of silence, 1 due to beam blockage, and 1 due to a combination of both), leaving 13 stations viable for subsequent analysis. The spatial distribution of the radar and the selected gauge stations is presented in Figure 1.

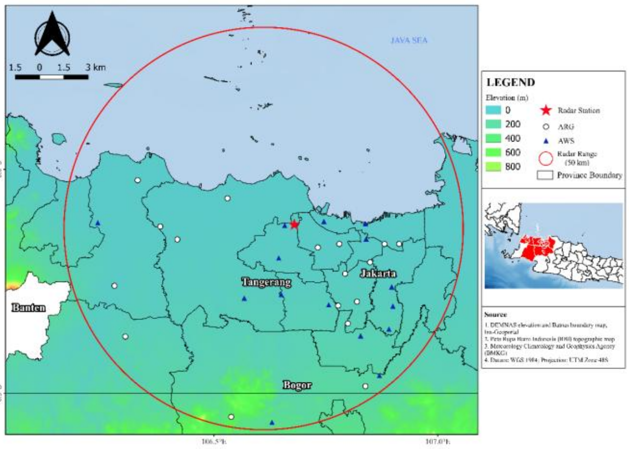

Figure 1. Study area showing the location of the Tangerang C-Band radar and the distribution of automatic rain gauge stations within the 50 km observation radius.

Data and Instruments

Two primary datasets support this research. The first consists of volumetric raw radar data (.vol) produced by the single-polarization EEC C-Band radar at Tangerang, recorded at 10-minute temporal resolution and obtained through an official data request submitted to Soekarno-Hatta Meteorological Station. The second dataset comprises hourly rainfall accumulation from 32 automatic rain gauges within the 50 km radar coverage, consisting of 17 Automatic Rain Gauges (ARG) and 15 Automatic Weather Stations (AWS), retrieved from the BMKG database.

Radar processing was carried out using the wradlib Python library executed through Google Colaboratory, covering clutter reduction, attenuation correction, and reconstruction of three-dimensional reflectivity into Constant Altitude Plan Position Indicator (CAPPI) products. Subsequent statistical computation, reflectivity-rainfall comparison, and Taylor Diagram generation were performed with Python scripts within the same environment.

Rain Gauge Quality Control and Rain-Type Classification

Before regression analysis, the 32 candidate stations were screened against two radar-geometry limitations: beam blockage and the cone of silence. The horizontal ground radius of the cone of silence was calculated following the geometric formulation of Doviak and Zrnić (2014) :

$$\boldsymbol{s} = \boldsymbol{Re'sin}^{-1}[(\boldsymbol{Rscos\theta})/(\boldsymbol{Re'} + \boldsymbol{H})]$$

with the corresponding slant range obtained from

$$\boldsymbol{Rs} = \sqrt{}[(\boldsymbol{Re'} + \boldsymbol{H})^2 - (\boldsymbol{Re'cos\theta})^2] - \boldsymbol{Re'sin\theta}$$

where s denotes the horizontal ground radius of the cone of silence boundary (km), Rs the slant range from radar to target (km), H the target height above the radar (km), θ the maximum antenna elevation angle (°), and Re' the effective earth radius, taken as 8,494.67 km using a standard refraction constant of k = 4/3 and a nominal earth radius of 6,371 km. Stations falling inside a blocked sector or within the calculated cone-of-silence radius were excluded from further processing, alongside stations with incomplete temporal records.

Retained rainfall events were sorted into three interaction categories between radar detection and gauge recording, following the scheme proposed by Hutapea et al. (2021), rainfall detected by radar but not recorded by the gauge (Type I), rainfall recorded by the gauge but undetected by radar (Type II), and rainfall registered by both instruments (Type III). Only Type III events were carried into the regression stage, since these represent the paired observations required to relate reflectivity to rain rate. Applying this classification across the 13 retained stations over the January-April 2024 period yielded a total of 21,101 Type III radar-gauge pairs. Of these, the convective subset (≥10 mm/hour) used for the regression presented in this study comprised 13,748 rainfall events. Hourly accumulated rainfall from the retained Type III events was then classified by intensity following the threshold established by Nzeukou and Sauvageot (2004), under which rain rate ≥10 mm/hour is designated convective.

Hourly accumulated rainfall from the retained Type III events was then classified by intensity following the threshold established by Nzeukou and Sauvageot (2004), under which rain rate ≥10 mm/hour is designated convective. This study isolates the convective subset for coefficient derivation, given its closer link to short-duration, high-intensity rainfall associated with urban flood risk in Jakarta. Convective rainfall values were converted to decibel units to allow linear regression against reflectivity on a logarithmic scale :

$$dBR = 10log_{10}(R)$$

Radar Data Processing

Raw volumetric data were converted from polar-coordinate .vol format into CAPPI products with 0.5 km horizontal pixel resolution across ten vertical levels spanning 0.5 to 5.0 km altitude, at 0.5 km vertical intervals, as illustrated in Figure 2. The highest reflectivity value across the ten vertical layers at each grid cell was retained to construct the Column Maximum (CMAX) product.

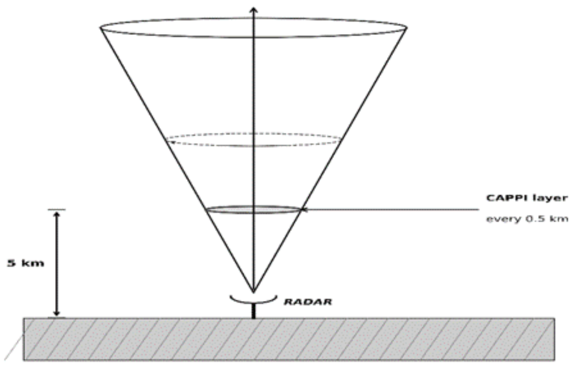

Figure 2. Vertical layer configuration of the CAPPI product used for CMAX extraction.

CMAX data were subsequently reprojected from polar to Universal Transverse Mercator (UTM) cartesian coordinates. For each selected gauge location, a 3×3 grid of surrounding CMAX pixels was extracted, with the center cell corresponding to the pixel nearest the gauge position, following the scheme shown in Figure 3.

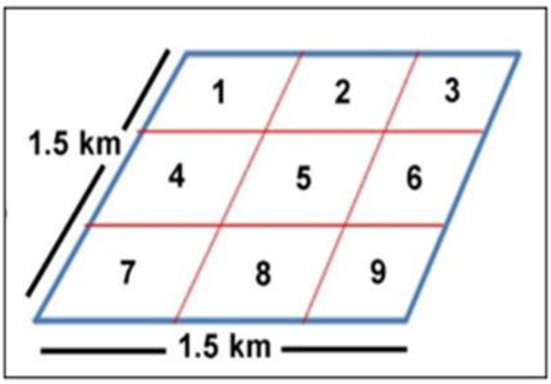

Figure 3. Grid extraction scheme applied to CMAX data at each rain gauge location.

Reflectivity values recorded at 10-minute intervals were averaged into hourly values to match the temporal resolution of the gauge data :

$$Zj = (1/n)\Sigma Zij$$

where Zj is the mean hourly reflectivity for hour j, and Zij is the 10-minute reflectivity value i within hour j.

Z-R Regression for Convective Rainfall

Paired dBZ and dBR values from the convective subset were regressed in logarithmic space to estimate the coefficients of the power-law relationship $Z = AR^b$, using the linearized form :

$$log(Z) = log(A) + b \cdot log(R)$$

where the intercept corresponds to log(A) and the slope corresponds to the exponent b. The resulting coefficients were converted back to the standard Z-R form for direct comparison against Marshall-Palmer and Rosenfeld Tropical.

Accuracy Verification

Estimation accuracy was assessed using a Taylor Diagram (Taylor, 2001), which jointly summarizes correlation coefficient, standard deviation, and root mean square error relative to the rain gauge observations treated as ground truth. RMSE was calculated as

$$RMSE = \sqrt{[(1/n)\Sigma(Y_i - \hat{Y}_i)^2]}$$

where Y_i is the observed value, $\hat{Y}_i$ the estimated value, and n the number of data pairs. Standard deviation of the estimated series was computed as

$$\sigma = \sqrt{[(1/n)\Sigma(X_i - X)^2]}$$

and the Pearson correlation coefficient as

$$r = \Sigma(Y_i - \bar{Y})(\hat{Y}_i - \bar{Y}*)/\sqrt{[\Sigma(Y_i - \bar{Y})^2\Sigma(\hat{Y}_i - \bar{Y}*)^2]}$$

Correlation values were interpreted according to the criteria in Table 1.

Table 1. Interpretation of the Pearson correlation coefficient (r)

Correlation Coefficient (r)	Interpretation
0.9 to 1.0 (or −0.9 to −1.0)	Very high correlation
0.7 to 0.9 (or −0.7 to −0.9)	High correlation
0.5 to 0.7 (or −0.5 to −0.7)	Moderate correlation
0.3 to 0.5 (or −0.3 to −0.5)	Low correlation
0.0 to 0.3 (or 0.0 to −0.3)	Negligible correlation

The complete processing sequence, from rain gauge quality control through radar reprojection to Taylor Diagram verification, is summarized in Figure 4.

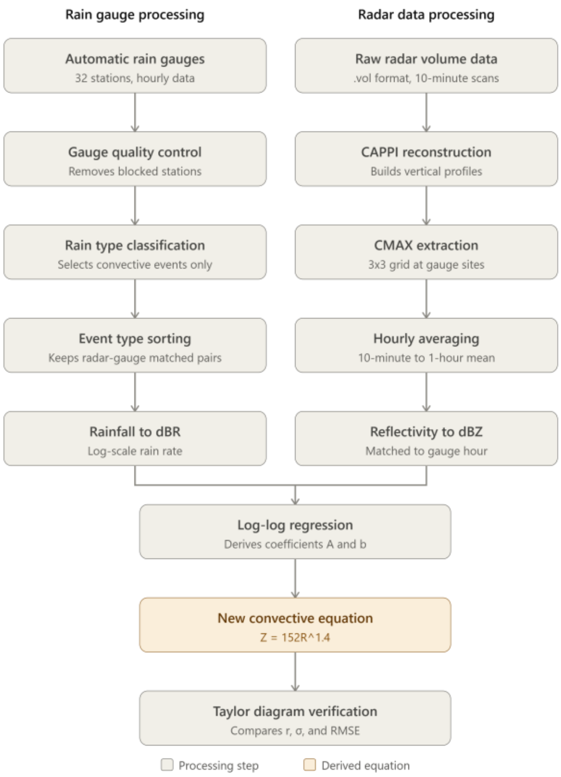

Figure 4. Flowchart of the data processing and verification procedure for the convective Z-R equation.

Result and Discussion

Regression Characteristics of the Convective Equation

Type III rainfall events with intensity at or above 10 mm/hour were isolated from the full dataset and paired as logarithmic reflectivity (dBZ) against logarithmic rainfall (dBR) for regression analysis, as shown in Figure 5.

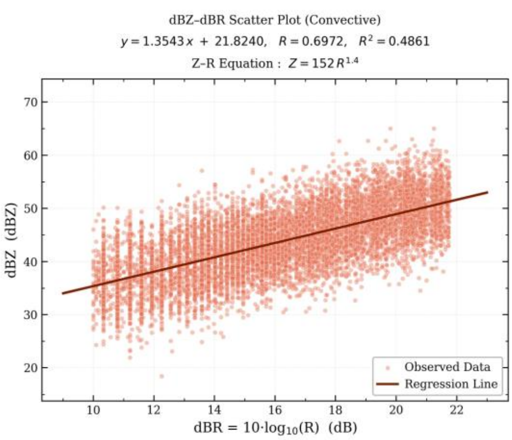

Figure 5. Scatter plot of dBZ against dBR for convective rainfall events, with the fitted regression line.

The fitted line follows dBZ = 21.8240 + 1.3543 dBR, yielding a Pearson correlation coefficient of 0.6972 and a coefficient of determination of 0.4861. Converting the intercept and slope into linear form produces the power-law relationship $Z = 152R^{1.4}$, where coefficient A = 152 derives from $10^{(21.8240/10)}$ and exponent b rounds from 1.3543. A correlation of 0.6972 falls into the moderate category under the interpretation scale in Table 1, noticeably lower than the very high correlations typically obtained when the same radar network's data are analyzed without separating rain type.

The spread of points around the regression line in Figure 5 is wider than a moderate R^2 alone would suggest. Near a rain rate of 31 mm/hour (approximately 15 dB), recorded reflectivity ranges from roughly 35 to more than 60 dBZ, a spread of 25 dBZ for a single rainfall value. Such dispersion is consistent with what convective microphysics predicts: active updrafts sustain droplet collision, coalescence, and breakup at the same time, so the drop size spectrum shifts continuously rather than settling into one stable form. Read this way, an R^2 of 0.4861 marks a practical ceiling for a single regression line applied to convective rainfall, not a weak physical link between reflectivity and rain rate. Coefficient A = 152 stays below both Marshall-Palmer (A = 200) and Rosenfeld Tropical (A = 250), meaning that at matched reflectivity, the local equation returns a higher rain rate estimate than either standard formula, in line with a drop population weighted toward smaller diameters typical of maritime tropical convection.

Accuracy Verification and Physical Significance

Independent verification against the 2024 observation record tests how closely $Z = 152R^{1.4}$ reproduces observed rainfall variability relative to the two standard equations, summarized in the Taylor diagram in Figure 6.

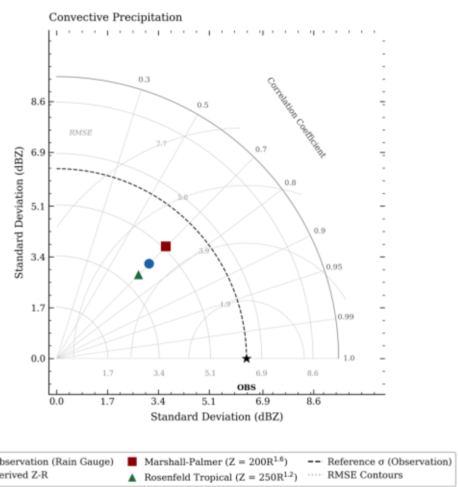

Figure 6. Taylor diagram comparing the estimation performance of the new convective equation, Marshall-

Palmer, and Rosenfeld Tropical against observed rainfall.

Observed convective rainfall carries a standard deviation of approximately 6.4 dBZ, while all three equations cluster between 3.0 and 3.7 dBZ, so each approach compresses the true variability of convective bursts to roughly half its observed magnitude. Root mean square error sits near 3.9 dBZ across all three, leaving little separation on error magnitude alone. Correlation is where the equations diverge: the new convective relationship reaches r ≈ 0.95, ahead of Marshall-Palmer at r ≈ 0.90, as summarized in Table 2.

Table 2. Verification statistics for convective rainfall estimation (Taylor diagram)

Equation	Correlation Coefficient (r)	RMSE (dBZ)
New convective equation ($Z = 152R^{1.4}$)	≈ 0.95	≈ 3.9
Marshall-Palmer ($Z = 200R^{1.6}$)	≈ 0.90	≈ 3.9

Rosenfeld Tropical shows a relatively high correlation, but among the three, its position is closest to the origin of the position diagram associated with the strongest emphasis on the estimated variability. Overall, this new equation occupies the most balanced position on the diagram, tracking temporal and spatial patterns of convective rainfall more accurately than Marshall-Palmer, while maintaining a broader range of observations than that maintained by Rosenfeld Tropical. Regressions based on rainfall distributions at mid-latitudes, such as the Marshall-Palmer model, lack a solid foundation for tracking the rapid intensity fluctuations characteristic of tropical convective cells, which provides a plausible explanation for their lower correlation in this dataset.

The shared gap between observed and modeled standard deviation across all three equations carries a practical implication beyond the statistics themselves. Since every formula tested understates the true variability of convective rainfall, each remains prone to underestimating the most intense bursts, precisely the rainfall regime most closely tied to flash flooding in a dense urban catchment like Jakarta. The correlation gain offered by $Z = 152R^{1.4}$, even without fully closing the variability gap, points to a locally calibrated coefficient as a steadier basis for convective QPE than either general-purpose formula currently in operational use.

Conclusion

This study derived a locally calibrated Z-R equation for convective rainfall at the Tangerang C-Band radar, expressed as Z=152R^1.4, using paired reflectivity and rain gauge observations collected between January and April 2024. The regression coefficient ($r = 0.6972$, $R^2 = 0.4861$) reflects the inherently wide drop size distribution spectrum that characterizes convective precipitation, rather than indicating a weak physical relationship between reflectivity and rain rate. Verification through the Taylor Diagram showed the new equation reproducing observed rainfall patterns more closely than Marshall-Palmer, reaching a correlation of approximately 0.95 against approximately 0.90, while preserving more of the natural rainfall variability than Rosenfeld Tropical. All three equations understated the true standard deviation of convective rainfall to a similar degree, pointing to a shared limitation of single-regression Z-R models under highly variable DSD conditions, yet the locally derived coefficient produced the most balanced performance among the three formulations tested.

These findings support adopting a regionally calibrated convective coefficient in place of the generic Marshall-Palmer and Rosenfeld Tropical equations for operational quantitative precipitation estimation at BMKG's Tangerang radar, given the close link between convective rainfall and flash flood risk across the Jakarta metropolitan area. Integrating the derived convective equation (Z=152R^1.4) into the coefficient input of BMKG's operational radar processing software, such as the Stratiform-Convective Classification (SCCL) module within Rainbow 5, would allow the system's existing real-time classification capability to be matched with region-specific coefficients rather than the generic defaults it currently relies on. For forecasters monitoring convective cells during extreme weather events, this closer match between classification and calibration translates into more reliable QPE output at the exact rainfall intensities most closely tied to urban flood risk, supporting faster and more confident early warning decisions. A longer observation window spanning a full annual cycle, capturing seasonal shifts in drop size distribution beyond the four-month period examined here, would help confirm the stability of this coefficient under a wider range of atmospheric conditions.

Acknowledgements

The author would like to express appreciation to Soekarno-Hatta Class I Meteorological Station, Tangerang, for granting access to the volumetric raw radar data (.vol) used throughout this research. Gratitude is also extended to the Meteorology, Climatology, and Geophysics Agency (BMKG) for providing hourly rainfall records from the automatic rain gauge network within the study area. This research was carried out as part of an undergraduate thesis at the Meteorology Study Program, Sekolah Tinggi Meteorologi Klimatologi dan Geofisika (STMKG), and appreciation is due to the supervisors and examining committee whose guidance shaped the analytical approach applied in this study. No external grant funding was received for this research.

References

Biondi, A., Facheris, L., Argenti, F., Cuccoli, F., Antonini, A., & Melani, S. (2024). Evaluation of quantitative rainfall estimation methods based on the integration of weather radar and rain gauge data. IEEE Geoscience and Remote Sensing Letters, 21, 1–5. https://doi.org/10.1109/lgrs.2024.3434650

Bringi, V. N., & Hendry, A. (1990). Technology of polarization diversity radars for meteorology. In Radar in Meteorology (pp. 153–190). Springer.

Dhiram, K., & Wang, Z. (2016). Evaluation on radar reflectivity-rainfall rate (ZR) relationships for Guyana. Atmospheric and Climate Sciences, 6(4), 489–499.

Doviak, R. J., & Zrnić, D. S. (2014). Doppler radar and weather observations. Academic Press.

Gou, Y., & Chen, H. (2021). Combining radar attenuation and partial beam blockage corrections for improved quantitative application. Journal of Hydrometeorology, 22(1), 139–153.

Hutapea, T. D. F., Permana, D. S., Praja, A. S., & Muzayanah, L. F. (2021). Modifikasi konstanta persamaan ZR radar Surabaya untuk peningkatan akurasi estimasi curah hujan. Jurnal Meteorologi dan Geofisika, 21(2), 91–97.

Kidd, C., Becker, A., Huffman, G. J., Muller, C. L., Joe, P., Skofronick-Jackson, G., & Kirschbaum, D. B. (2017). So, how much of the Earth's surface is covered by rain gauges? Bulletin of the American Meteorological Society, 98(1), 69–78.

Kusuma, I. K. N. A., & Wardoyo, E. (2018). Uji keakurasian estimasi hujan menggunakan hubungan Z-R untuk tipe awan hujan konvektif dan stratiform di Jakarta. Megasains, 9(1), 33–40.

Lakkham, M. (2017). Determining the appropriate altitude to improve accuracy in rainfall estimation from radar reflectivity data. Journal of Physics: Conference Series, 901(1), 012045.

Marshall, J. S., & Palmer, W. M. (1948). The distribution of raindrops with size. Journal of Meteorology, 5, 165–166.

Mocva-Kurek, R. K., Pedrozo-Acuña, A., & Rico-Ramírez, M. A. (2025). Spatial heterogeneity of drop size distribution and its implications for the Z-R relationship in Mexico City. Atmosphere, 16(5), 585.

Mundir, M. (2012). Statistik pendidikan: Pengantar analisis data untuk penulisan skripsi dan tesis. STAIN Jember Press.

Notaroš, B. M. (2022). Polarimetric weather radar: An overview of principles and applications. IEEE Antennas and Propagation Magazine, 64(5), 43–54.

Nzeukou, A., & Sauvageot, H. (2004). Raindrop size distribution and radar parameters at Cape Verde. Journal of Applied Meteorology, 43, 90–105.

Romatschke, U., & Dixon, M. (2022). 3D convective/stratiform echo type classification and convectivity: Application to GPM and CloudSat radar reflectivities. Collective Madison Meeting. American Meteorological Society.

Rosenfeld, D., Wolff, D. B., & Atlas, D. (1993). General probability-matched relations between radar reflectivity and rain rate. Journal of Applied Meteorology, 32, 50–72.

Sahlaoui, Z., & Mordane, S. (2019). Radar rainfall estimation in Morocco: Quality control and gauge adjustment. Hydrology, 6(2), 41.

Syafira, S. A., Zahroh, N. F., Dewi, S., & Renggono, F. (2021). Karakteristik butir air hujan permukaan dan lapisan atas atmosfer pada puncak musim hujan di Tangerang Selatan. Jurnal Sains & Teknologi Modifikasi Cuaca, 22(1), 9–16.

Talumassawatdi, R., Lursinsap, C., & Yin, Y. (2016). Adaptive estimation of local rainfall from radar intensity using rule-based approach on temporal and spatial data. Chiang Mai Journal of Science, 43(3), 643–660.

Taylor, K. E. (2001). Summarizing multiple aspects of model performance in a single diagram. Journal of Geophysical Research, 106, 7183–7192.